

Electronic Supplementary Information

Supramolecular Assembly of Graphene with Functionalized Poly(Fluorene-*alt*-phenylene). The Role of the Antraquinone Pendant Groups.

Marta Castelaín, Horacio J. Salavagione, Rafael Gómez, José Luis Segura

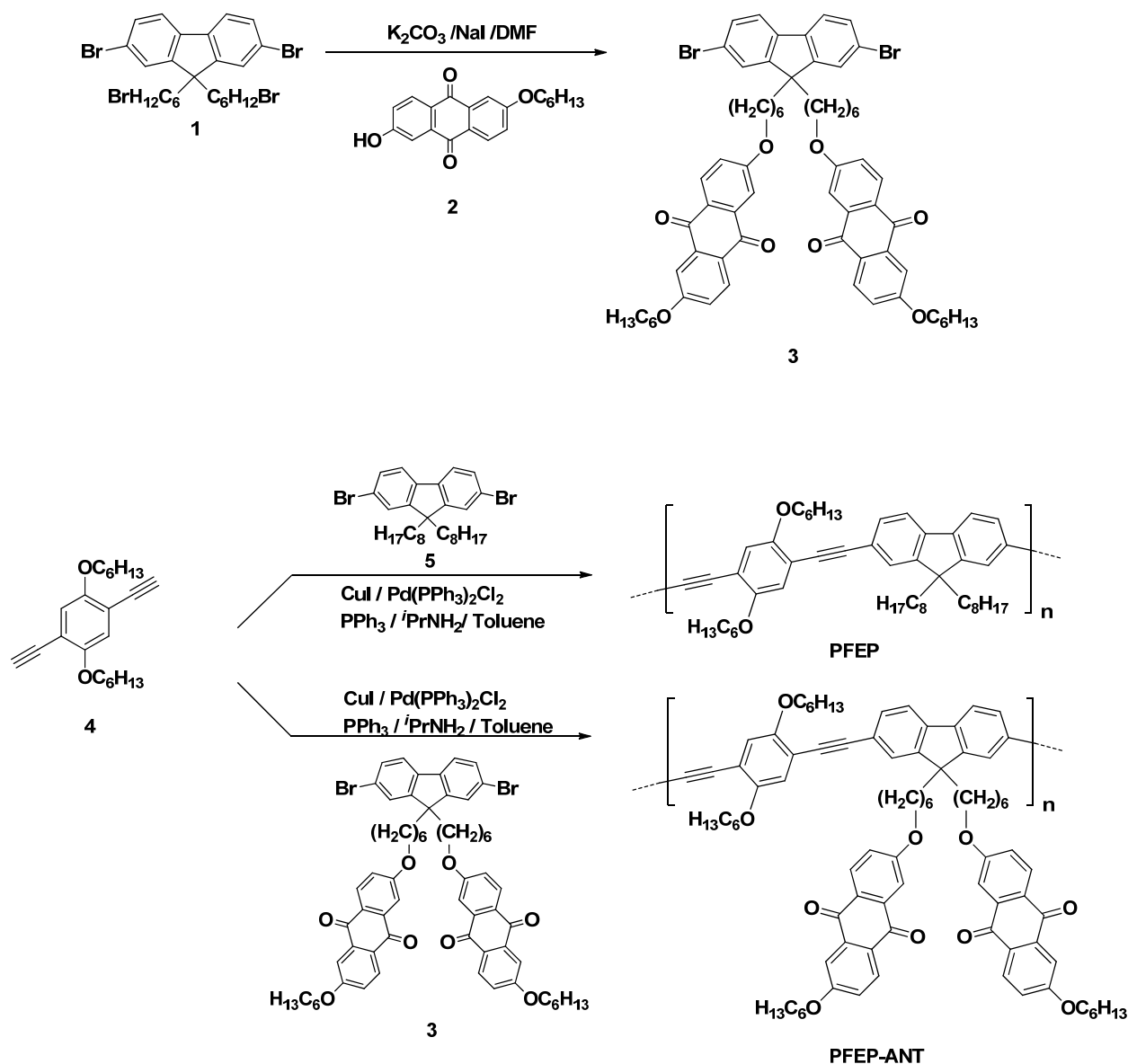
Experimental Details

Materials. The synthetic procedures for **PFEP** and **PFEP-ANT** are shown in Scheme S1. The reagents 2,7-dibromo-9,9-bis(6'-bromohexyl)fluorene (**1**),¹ 2-hexyloxy-6-hydroxy-9,10-antraquinone (**2**),² 1,4-diethynyl-2,5-dihexyloxybenzene³ (**4**) were prepared following previously reported synthetic procedures. All other chemicals were purchased from commercial sources and used as received without further purification. Solvents and reagents were dried by the usual methods prior to use and typically used under inert gas atmosphere.

Synthesis of monomer 3. To a solution of 2-hexyloxy-6-hydroxy-9,10-antraquinone (**2**) (400 mg, 1.23 mmol) in 60 mL of anhydrous DMF, potassium carbonate (510 mg, 3.69 mmol), 2,7-dibromo-9,9-bis(6'-bromohexyl)fluorene (**1**) (266 mg, 0.41 mmol) and a catalytic amount of sodium iodide were added under argon atmosphere. The mixture was heated at reflux for 48 hours. The crude was allowed to reach room temperature and treated with a 1N HCl aqueous solution. The resulting mixture was extracted with dichloromethane and the combined organic fractions dried over MgSO₄ and evaporated under vacuum. The remaining residue was purified by column chromatography (silica gel, dichloromethane/ethyl acetate 98/2) to give monomer **3** as a yellow solid (86%). M.p.: 71-72 °C (dichloromethane/ethyl acetate). ¹H-NMR (300 MHz, CDCl₃), δ (ppm): 7.98 (dd, 4H, *J* = 8.6, 3.8 Hz, *Ant*), 7.47 (d, 2H, *J* = 2.6 Hz), 7.42 (d, 2H, *J* = 2.6 Hz), 7.28 (m, 6H), 6.98 (dd, 2H, *J* = 8.6, 2.5 Hz), 6.94 (dd, 2H, *J* = 8.6, 2.5 Hz), 3.92 (t, 4H, *J* = 6.6 Hz, -CH₂-O), 3.81 (t, 4H, *J* = 6.4 Hz, -CH₂-O), 1.81-1.71 (m, 4H, -CH₂-), 1.69-1.57 (m, 4H, -CH₂-), 1.52-1.39 (m, 4H, -CH₂-), 1.35-1.22 (m, 4H, -CH₂-), 1.22-1.11 (m, 8H, -CH₂-), 1.11-1.01 (m, 8H, -CH₂-), 1.01-0.89 (m, 4H, -CH₂-), 0.77-0.67 (t, 6H, *J* = 7.0 Hz, -CH₃). ¹³C-NMR (75 MHz, CDCl₃), δ (ppm): 182.3 (C=O), 164.1 (C_{Ar}-O), 152.3 (C_{Ar}-O), 139.1, 135.8, 130.4, 129.6, 127.0, 126.2, 121.6, 121.3, 120.9, 120.9, 110.5, 68.8 (-CH₂-O-), 55.6 (C_{bridge}), 40.1 (CH₂-C_{bridge}), 31.5, 29.7, 29.5, 29.0, 28.9, 25.6, 23.6, 22.6, 14.0. FT-IR, v

(cm⁻¹): 2930, 2858, 1669 (C=O), 1589 (C=C), 1303, 1230, 740. MS (MALDI-TOF) (*m/z*): 1138 (M⁺+1). Microanalysis. Calc. for C₆₅H₆₈Br₂O₈: C, 68.66 %; H, 6.03 %. Found: C, 68.14 %; H, 6.08 %.

Scheme S1. Synthetic schemes for PFEP and PFEP-ANT.



Synthesis of PFEP. A mixture of 2,7-dibromo-9,9-dioctylfluorene (**5**) (123 mg, 0.2 mmol), 1,4-diethynyl-2,5-dihexyloxybenzene (**4**) (75 mg, 0.2 mmol), bis(triphenylphosphine)palladium (II) dichloride (8 mg, 6.5·10⁻³ mmol), copper iodide (9 mg, 0.05 mmol), triphenylphosphine (60 mg, 0.2 mmol) and diisopropylamine (3.0 mL) in 50 mL

of deareated anhydrous toluene was heated at reflux for 72 hours under argon atmosphere. The reaction mixture was allowed to cool down to room temperature and slowly added into methanol to give an orange precipitate. The solid was collected, dissolved in chloroform, and precipitated out of methanol again. The polymer was further purified by washing with acetone in a Soxhlet apparatus for 24 h to remove small molecules, oligomers, and catalyst residues. The final product was dried under vacuum, to give polymer **PFEP** as an orange solid in 90% yield. ¹H-NMR (400 MHz, CDCl₃), δ (ppm): 7.59-7.43 (br m, 4H, *Fl*), 7.38-7.32 (m, 2H, *Fl*), 6.96 (s, 2H, *Ph*), 3.93 (m, 4H, C_{Ph}-O-CH₂-), 2.04 (s, 4H, -CH₂-C_{bridge}), 1.98-1.75 (br m, 8H, -CH₂-), 1.63-1.42 (br m, 4H,-CH₂-), 1.42-1.30 (br m, 8H,-CH₂-) 1.25 (s, 12H, -CH₂-), 1.22-1.16 (m, 4H,-CH₂-), 1.14-1.00 (m, 4H,-CH₂-), 0.92 (br s, 6H, -CH₃), 0.82 (t, 6H, -CH₃). ¹³C-NMR (100 MHz, CDCl₃), δ (ppm): 153.0 (C_{Ph}-O), 147.9, 147.1 (C_{Ph}-O), 134.8, 133.1, 131.0, 127.8, 117.3 (C_{Ph}), 115.0 (C_{Ph}), 109.4, 104.1, 97.5 (C≡C), 90.6 (C≡C), 71.8 (-CH₂-O-), 69.1 (-CH₂-O-), 56.2 (C_{bridge}), 31.6 (-CH₂-), 31.2, 31.0, 30.9, 29.4, 29.1, 29.0, 28.8, 28.6, 28.4, 25.8, 24.9, 22.8, 22.0, 13.6 (-CH₃), 13.4 (-CH₃). FT-IR, ν (cm⁻¹): 2929, 2854, 1496 (C=C), 1472, 1388, 1274, 1214, 1027, 864, 804. GPC (vs PS) M_w = 8627 g.mol⁻¹; M_n = 23390 g.mol⁻¹; pd = 2.71

Polymer PFEP-ANT. The key building block in the synthesis of the conjugated functionalized polymer **PFEP-ANT** (**1**) is 2,7-dibromo[9,9-bis(6-[(6-hexyloxy-9,10-anthraquinon-2-yl)oxy]hex-1-yl)]fluorene (compound 3 in Scheme S1), a monomer that is functionalized with two pendant 9,10-anthraquinone units, to enhance the π-π stacking ability between the polymer and graphene. On the other hand, long non-conjugated alkyl linkers are introduced between the polymer backbone and the 9,10-anthraquinone moiety to enhance the solubility and processability of the polymer.

A mixture of monomer **3** (171 mg, 0.15 mmol), 1,4-diethynyl-2,5-dihexyloxybenzene (**4**) (50 mg, 0.15 mmol), bis(triphenylphosphine)palladium (**II**) dichloride (5 mg, 4.4·10⁻³ mmol), copper iodide (6 mg, 0.03 mmol), triphenylphosphine (30 mg, 0.11 mmol) and diisopropylamine (2.0 mL) in 35 mL of deareated anhydrous toluene was heated at reflux for 72 hours under argon atmosphere. The reaction mixture was allowed to cool down to room temperature and slowly added into methanol to give an orange precipitate. The solid was collected, dissolved in chloroform, and precipitated out of methanol again. The polymer was further purified by washing with acetone in a Soxhlet apparatus for 24 h to remove small molecules, oligomers, and catalyst residues. The final product was dried under vacuum to afford polymer **PFEP-ANT** as an orange solid in 93 % yield. ¹H-NMR (400 MHz, CDCl₃), δ

(ppm): 8.25-8.15 (m, 4H, *Ant*), 7.69-7.48 (m, 6H, *Fl*), 7.41-7.32 (m, 4H, *Ant*), 7.23-7.11 (m, 4H, *Ant*), 6.97 (s, 2H, *Ph*), 4.07 (t, 4H, $J = 6.4$ Hz, -CH₂-O-), 3.95 (t, 4H, $J = 6.4$ Hz, -CH₂-O-), 3.69 (m, 4H, C_{Ph}-O-CH₂-), 2.09-1.89 (m, 4H, -CH₂-C_{bridge}), 1.88-1.78 (br m, 4H, -CH₂-), 1.72-1.43 (br m, 16H, -CH₂-), 1.40-1.31 (br m, 8H, -CH₂-), 1.29-0.98 (br m, 20H, -CH₂-), 0.92 (t, 6H, $J = 6.9$ Hz, -CH₃), 0.85 (t, 6H, $J = 6.9$ Hz, -CH₃). ¹³C-NMR (100 MHz, CDCl₃), δ (ppm): 182.3 (C=O), 182.2 (C=O), 164.0 (C_{Ant}-O), 163.9 (C_{Ant}-O), 154.8 (C_{Ph}-O), 152.2 (C_{Ph}-O) 139.1, 135.8, 130.3, 129.6, 129.5, 126.9, 126.1, 121.5, 121.2, 120.9, 120.8, 110.5 (C≡C), 110.4 (C≡C), 68.8 (-CH₂-O-), 68.6 (-CH₂-O-), 51.0 (C_{bridge}), 40.1 (-CH₂-C_{bridge}), 31.6 (-CH₂-), 31.5, 31.4, 29.6, 29.4, 29.0, 28.9, 28.8, 25.6, 25.5, 23.6, 23.5, 22.6, 22.5, 14.1 (-CH₃), 13.9 (-CH₃). FT-IR, ν (cm⁻¹): 2929, 2860, 1670 (C=O), 1590 (C=C), 1496, 1472, 1427, 1388, 1302 (C-O), 1214, 1081, 1027, 884, 860, 745. SEC (vs PS) $M_w = 25958$ g.mol⁻¹; $M_n = 61386$ g.mol⁻¹; pd = 2.36

Preparation of PFEP-ANT/Grf

To prepare the **PFEP-ANT**/graphene dispersions in NMP, 6.5 mg of **PFEP-ANT** and 1.3 mg of electrochemically expanded graphite⁴ powder were mixed by sonication during 30 min in 10 mL of NMP. The dispersion was centrifuged for 10 min at 7000 rpm and was allowed to stand overnight. The phases were separated to give a solid powder (**PFEP-ANT/Grf**) which was dried at 40°C under vacuum and the supernatant (**s-PFEP-ANT/Grf**) which was pipetted into another vial, producing a solution of discrete polymer-graphene complexes. The Eppendorf vial on the right side of Figure S1 shows Tyndall effect due to the effective dispersion of graphene particles being this a first evidence of interactions between the **PFEP-ANT** and graphene.

The same procedure was repeated using graphite as source of graphene and the solid product was named **PFEP-ANT/G**.

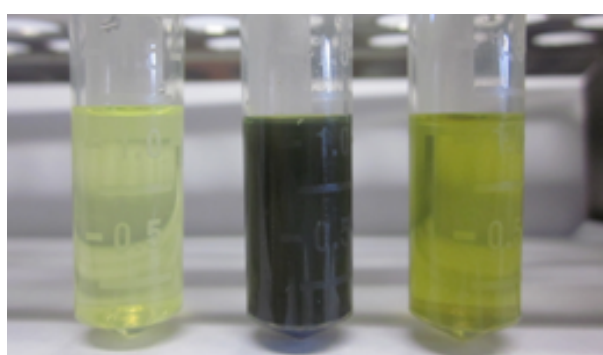


Fig. S1. From left to right: solution of **PFEP-ANT** polymer in NMP; dispersion of expanded graphite in the latter solution before centrifugation and dispersion of **PFEP-ANT/Grf** after separation.

Characterization.

NMR spectra were recorded on a Varian 400 or 500 at 25 °C, and chemical shifts are reported in ppm using the solvent as reference. The splitting patterns are designated as follows: s = singlet, d = doublet, t = triplet, m = multiplet, dd = doublet of doublets and the assignments are *Ant* (anthraquinone), *bridge* (fluorene C-9), *Fl* (fluorene) and *Ph* (phenyl). Mass spectra were recorded with a Varian Saturn 2000 and with a MALDI-TOF MS Bruker Reflex 2. Melting points were measured with an electrothermal melting point apparatus and are uncorrected. Elemental analyses were performed on a Perkin-Elmer EA 2400.

Electrochemistry. Cyclic voltammetry experiments were performed with a computer-controlled Autolab PGSTAT 302 potentiostat in a three electrode single-compartment cell (5 mL). The platinum working electrode consisted of a platinum wire with a surface of $A = 0.785 \text{ mm}^2$, which was polished down to 0.5 µm with Buehler polishing paste prior to use in order to obtain reproducible surfaces. The counter electrode consisted of a platinum wire and the reference electrode was a Ag/AgCl secondary electrode. For these measurements, concentrations of $5 \times 10^{-3} \text{ mol L}^{-1}$ of the electroactive polymer was used in freshly distilled and deaerated dichloromethane (HPLC, Aldrich) and 0.1 M tetrabutylammonium hexafluorophosphate (TBAHFP, Fluka), which was twice recrystallized from ethanol and dried under vacuum prior to use.

Samples for electrochemical measurements were prepared as follow: for **PFEP-ANT/Grf**, 2 mg of solid were dispersed in 5 mL of CH_2Cl_2 , while for the **s-PFEP-ANT/Grf** 3 mL of the supernatant of **PFEP-ANT/Grf** were added to 7 mL of the electrolyte solution.

For **PFEP-ANT/G** the solid was treated as in the case of **PFEP-ANT/Grf**.

UV/Vis absorption and photoluminescence. UV-vis absorption and photoluminescence spectra were recorded with a PerkinElmer Lambda 900 spectrometer. Diluted dichloromethane solutions ($\sim 10^{-6} \text{ M}$) were used, with an excitation wavelength corresponding to the absorption maxima. The fluorescence spectra were normalized with respect to the optical density of the samples.

Scanning Electron Microscopy.

SEM measurements samples were prepared as follow: a few µL of dispersed samples were drop-casted onto a flat strip of polyethylene and dried under vacuum. The samples-covered PE

substrates were cryo-fractured and coated with ca. 5nm Au/Pd overlayer and images of both top and side were collected with a Philips XL30 SEM equipment.

Raman spectroscopy

Confocal Raman measurements were made in the Raman Microspectroscopy Laboratory of the Characterization Service in the Institute of Polymer Science & Technology, CSIC. A Renishaw InVia Reflex Raman system (Renishaw plc., Wotton-under- Edge, UK) was used employing a grating spectrometer with a Peltier-cooled charge-coupled device (CCD) detector, coupled to a confocal microscope. All spectra were processed using Renishaw WiRE 3.2 software. The Raman scattering was excited using an Argon ion laser wavelength of 514.5 nm. The laser beam was focused on the sample with a 100· microscope objective (N.A. = 0.85), with a laser power at the sample of 62mW.

Results.

After centrifugation, well-dispersed few layer graphene dispersions are obtained. Characteristic Raman spectra of multiple and few layer graphene (FLG) were observed, as could be determined by the analysis of the second order 2D peaks arising from the zone boundary phonons⁵ (Fig S2). Also, the low intensity of the disorder-induced D band at 1350 cm⁻¹ indicates that the graphene laminates did not suffer important damages during the dispersion process (Fig S2). Usually, Raman spectra of this kind of conjugated polymer are hard to collect due to its strong fluorescence band. The good quality of the spectra (relatively good baseline) is an indirect evidence of effective polymer/graphene interactions that produces a quenching of the **PFEP-ANT** fluorescence.

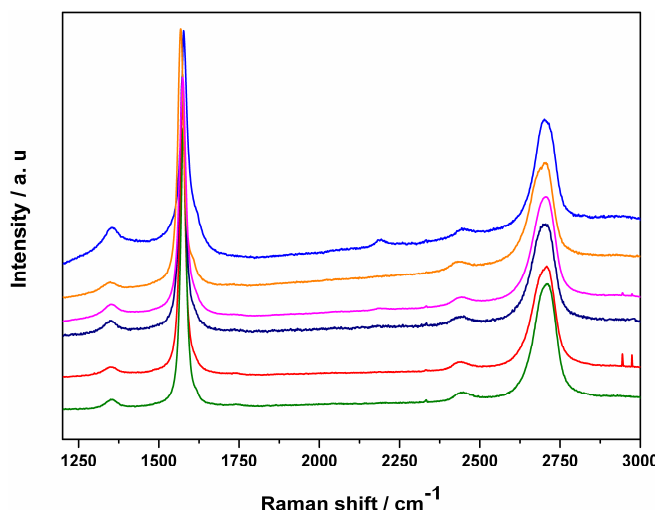


Fig S2. Representative spectra from different flakes of PFEP-ANT/Grf.

The fingerprint of this kind of conjugated polymers is their electronic behaviour since their absorption and emission spectra are sensible to the presence of donor/acceptor groups. Regarding the results in Cl_2CH_2 we collected absorption spectra in more polar solvents. The UV-Vis spectra collected in NMP and DMF show almost identical features for **PFEP-ANT** and **PFEP-ANT/Grf** (Fig S3). In these solvents, the displacement of the low energetic band of the **ANT** with graphene is imperceptible. Therefore, no correlation with the solvent polarity or other parameter as the surface energy can be extracted.

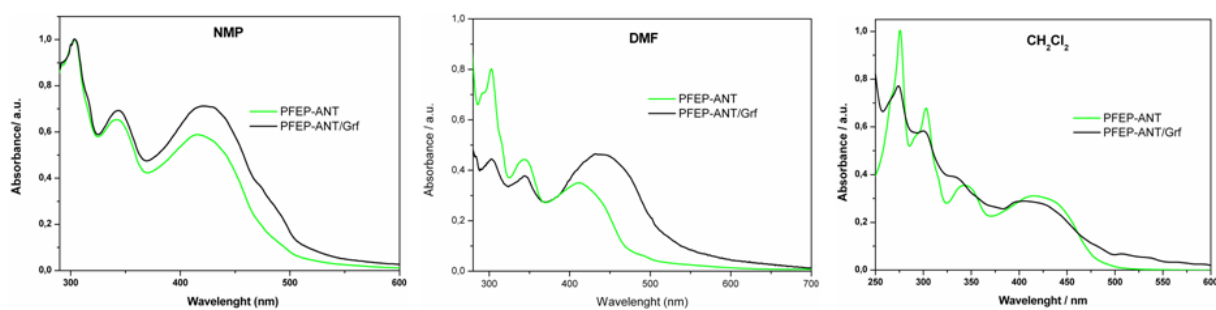


Fig. S3. Absorption spectra of **PFEP-ANT** and **PFEP-ANT/Grf** in different solvents.

However, it seems that PL of the polymer depends on the surface energy of the solvent as the PL of **PFEP-ANT** is totally quenched in Cl_2CH_2 , 95 % quenched in DMF but in NMP it

retains ca. 62% of the original PL (Fig S4, Table S1). These results could not be only explained by a solvent polarity effect, but are also related to its affinity for graphene⁶ in terms of solvent surface energy matching to the cohesive energy of graphene sheets.⁷ In other words, when **PFEP-ANT/Grf** is dispersed in NMP, a good solvent for dispersing graphene, the graphene “solvation” could cause that the graphene is “far away” from the **PFEP-ANT** backbone whose properties are not or weakly affected. However, when **PFEP-ANT/Grf** is dispersed in Cl_2CH_2 or DMF, worse solvents for graphene, it is “repelled” by the solvent adopting the most stable configuration in this landscape that is the association with **PFEP-ANT**.

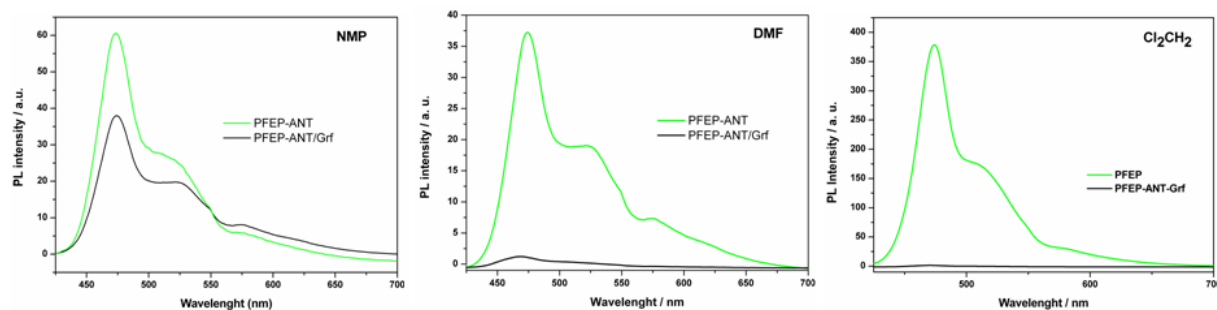


Fig. S4. PL emission spectra of **PFEP-ANT** and **PFEP-ANT/Grf** in different solvents.

Table S1. Solvent parameters, quenching of graphene on the PL of **PFEP-ANT** and displacements of the ANT redox peak in **PFEP-ANT/Grf**

Solvent	Surface Energy at 20°C ξ mJ.m ⁻²	Polarity	PL quenching of PFEP-ANT / %	Shift of ANT reduction peak mV
ACN	48.4	5.8		480
Cl_2CH_2	57.4	3.1	99.4	710
DMF	66.4	6.4	95	535
NMP	69.4	6.0	38	

ξ The cohesive energy for graphene sheets in graphite is around 70-80 mJ.m⁻² according to ref. 6 and 7.

Fig. S5 shows SEM morphological characterization of **PFEP-ANT/Grf** samples. The top-view of **PFEP-ANT/Grf** displays an almost uniform film composed of large size graphene sheets without important aggregation. Meanwhile, the side-view image of the same film shows densely-packed layered structures with approximately 800 nm thick.

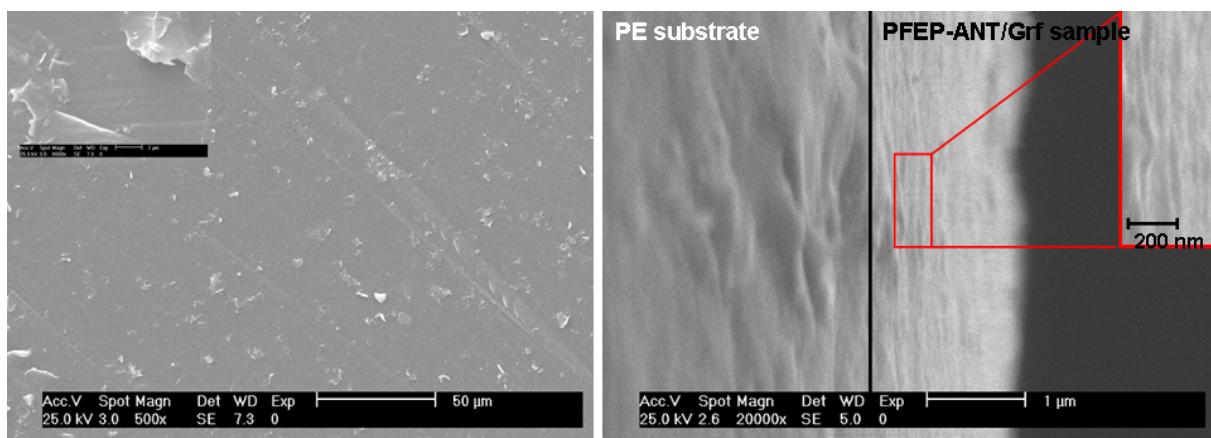


Fig. S5. Top-view (left) and side-view (right) of a thin film of **PFEP-ANT/Grf** casted onto a PE trip. Insets show magnification views.

Because of the striking results of CV in dichloromethane we have carried out the same experiments in different solvents, e.g. ACN and DMF, with 0.1 M TBAHFP as supporting electrolyte (Fig S6).

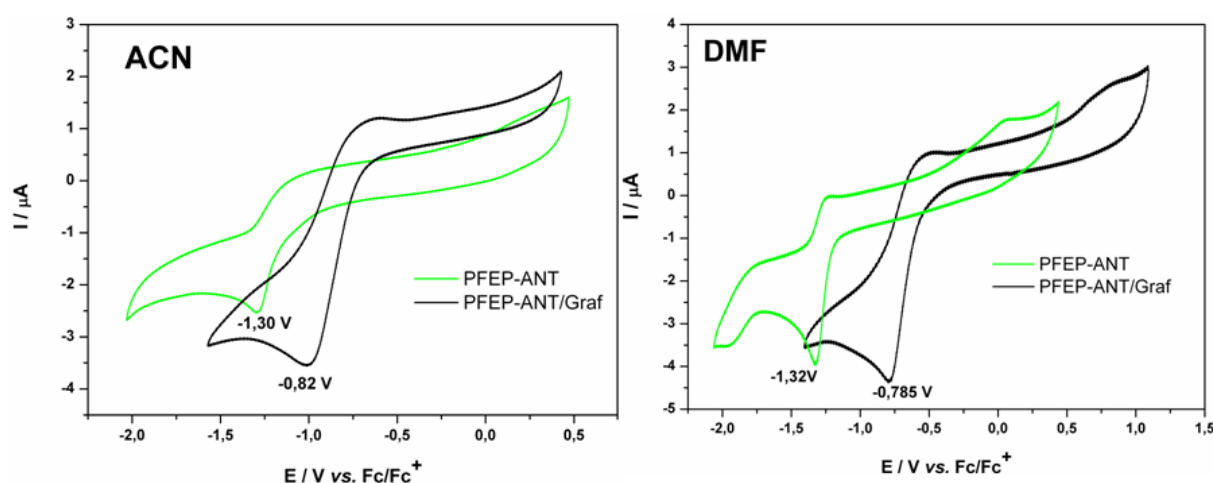


Fig S6. Cyclic voltammograms of **PFEP-ANT** and **PFEP-ANT/Grf** in different solvents.
Supporting electrolyte = 0.1 M TBAHFP, scan rate = 100 mV.s⁻¹

In both cases, the reduction peak of the ANT displaces to less negative potentials when graphene is present as it was observed in dichloromethane solutions (Table S1). However, the displacements are lower than in dichloromethane (table S1) and therefore some influence of the solvent should be considered. The relative shift of the reduction wave of the ANT moiety in different solvents must be influenced not only for the solvent polarity but also by the solvent surface energy as demonstrated by PL results. Nevertheless, it is clear that the presence of

graphene in any solvent facilitates the reduction of the ANT groups likely due to assembly of PFEP-ANT onto graphene sheets, which leads to some stacking.

We have also analyzed the role of the supporting electrolyte based in the ability of the anion radical of the ANT to form ion pairs.¹² Since the ion pairing effect is more evident when using alkali metals with small cationic radius, different amounts of lithium perchlorate were added to the PFEP-ANT/Grf containing ACN/TBAHFP solutions. Although the CVs were hard to record due likely to the formation of PFEP-ANT-Li solids onto the electrode surface, we perceived a slight variation of the ANT peak with the concentration of lithium (Figure S7). However, the magnitude of this shift is much less than that caused by the presence of graphene.

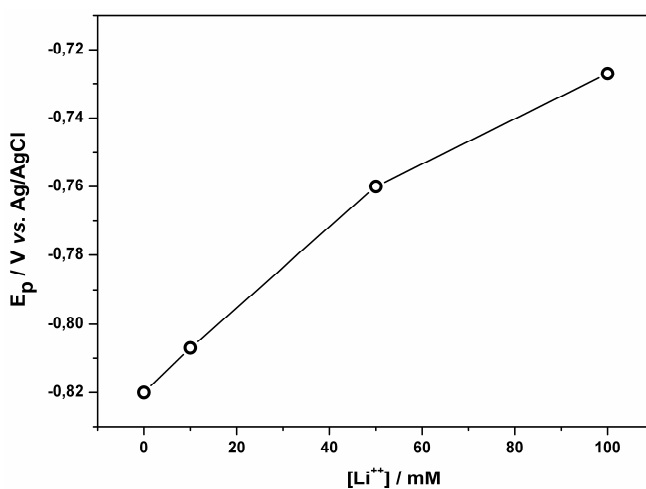


Fig. S7. Plot representing the variation of the reduction peak potential of ANT with the concentration of lithium cation.

Summarizing, although the solvent and the electrolyte can facilitate the reduction of ANT, the magnitude of these effects is very small related to the effect produced by the graphene.

References

-
- ¹ G. Zhou, G. Qian, L. Ma, Y. Cheng, Z. Xie, L. Wang, X. Jing, F. Wang, *Macromolecules*, 2005, **38**, 5416.
- ² J. L. Segura, R. Gómez, R. Blanco, E. Reinold, P. Bäuerle, *Chem. Mater.*, 2006, **18**, 2834.
- ³ R. Giesa, R. C. Schulz, *Makromol. Chem.*, 1990, **191**, 857.

-
- ⁴ G. M. Morales, P. Schifani, G. Ellis,C. Ballesteros, G. Martínez, C. Barbero, H. J. Salavagione, *Carbon*, 2011, **49**, 2809.
- 5 A.C. Ferrari, J. C. Meyer, V. Scardaci, C. Casiraghi, M. Lazzeri, F. Mauri, et al., *Phys Rev Lett* 2006, **97**, 187401.
- 6 R. Zacharia, H. Ulbricht, T. Heertel, *Phys Rev. B.*, 2004, **69**, 1545406.
- 7 Y. Hernandez, V. Nicolosi, M. Lotya, F. M. Blighe,Z. Sun Z, et al., *Nat. Nanotechnol.*, 2008,**3**,563.